

Simulation of structural vibrations induced by a moving load on railway tracks

Klaus Friedrich* and Nawawi Chouw**

* Dr.-Ing., Ruhr University Bochum, Department of Civil Engineering, Bochum, Germany

** Dr.-Ing., Associate Professor, Faculty of Environmental Science and Technology, Okayama University, Okayama 700-8530, Japan

A numerical approach for a simulation of the effect of moving loads on the vibration of a railway track and the vibration of a structure in the surrounding of the track is presented. Comparative analyses are performed. The rails, sleepers, elastic pads as well as the structure in the surrounding are described by finite elements, and the ballast and subsoil by boundary elements. The simulation is performed in the frequency domain. The investigation indicates that the speed of a moving load has a significant influence on the track and ground vibrations. The results show that in order to obtain a more realistic characteristic of the structural response to the ground motions it is not enough just to consider the vertical component of the ground motions.

Key Words: Moving load, soil-structure system, FE-BEM, Simulation, railway track, induced vibration

1. Introduction

Many investigations of the effect of ground motions focus on earthquakes as the vibration source. The reason is that major earthquakes often cause spectacular damage to structures, and lead to a multitude of victims. Vibrations due to human activities more and more become topic of many investigations recently. This is because people are more aware of their life quality. A collection of works on the effect of human-induced vibration is given in the proceedings of the international meeting on wave propagation, moving load and vibration reduction WAVE2000¹⁾ and WAVE2002²⁾.

In the case of moving loads like heavy trucks or high-speed trains the induced vibrations become more annoyance the larger the magnitude, the higher the speed of the moving load, and the closer the distance of the observation location from the vibration source is. The influence of a moving source is determined not only by the characteristic of the source, and the dynamic property of the considered structures, but it is also defined by the characteristic of the subsoil.

Many research works have been performed on the dynamic behaviour of the railway tracks, e.g. Krylov³⁾, Pan et al.⁴⁾, Petyt and Jones⁵⁾ and Lefeuvre-Mesgouez⁶⁾. In the investigation of ground vibrations Hirschauer⁷⁾ applied the Green's function for modeling the ground with the help of the

thin layer method developed by Waas⁸⁾ and Kausel⁹⁾. Mohammadi and Karabalis¹⁰⁾ used the full space fundamental solution BEM and a finite element method in their investigation of interaction between tracks and subsoil. The ties are assumed to be rigid. Effects of a moving load on track or ground vibrations have been performed, for example, by Zhu and Law¹¹⁾, Savin¹²⁾, Chen et al.¹³⁾, Barros and Luco¹⁴⁾ and Yang et al.¹⁵⁾.

Investigation on the effect of a moving load on a railway track on the ground as well as on a structure in the neighbourhood as performed in this study, however, is still very limited. In order to introduce the significance of the speed of the moving load, the response of the ground surface to a moving load on the ground is considered first without the railway track. For the simulation of the wave propagation from the moving source into the surrounding a three dimensional model is used. In the subsequent investigation the railway track is taken into account.

2. Railway tracks, subsoil and neighbouring building

In the first part of the study the ground vibration is caused by a load, moving directly on the ground surface. The ground is modeled by a boundary element method in the time domain, and a full-space fundamental solution is applied. The numerical

formulation is given by Pflanz^{16, 17}.

In the second part the influence of the railway track on the ground vibration as well as on the response of a frame structure in the vicinity of the track is considered as indicated in Fig. 1. The rails, the sleepers, and elastic pads in between, as well as the neighbouring structure with its foundations are described by finite elements. The ballast and the subsoil are modeled by boundary elements. The numerical formulation is performed in the frequency domain. By using the substructure technique we obtain the dynamic stiffness $\tilde{\mathbf{K}}$ of the whole system. After transforming the load into the frequency domain we can then determine the response of the ground to the moving load by multiplying $\tilde{\mathbf{P}}$ with the inverse of the dynamic stiffness matrix $\tilde{\mathbf{K}}$. The tilde indicates the vector or matrix in the frequency domain. A transformation of the results into the time domain provides us with the time history of the ground vibrations \mathbf{u} . The response of the neighbouring structure can be determined in the same procedure.

In order to describe the wave propagation from the interface between the sleepers and the ballast to the surrounding region we transform the wave equation and obtain the equation in the frequency domain.

$$\rho[(c_p^2 - c_s^2)\tilde{u}_{i,ik} + c_s^2\tilde{u}_{k,ii} - \omega^2\tilde{u}_k] = -\tilde{f}_k, \quad (1)$$

where \tilde{u}_k and \tilde{f}_k are the complex displacement and the amplitude of a harmonic load with the frequency ω , respectively.

$$c_p = \sqrt{\frac{\lambda + 2\mu}{\rho}} \text{ and } c_s = \sqrt{\frac{\mu}{\rho}} \text{ are the compressive and}$$

shear wave velocity, respectively, and $i = k = 1, 2, 3$. By assuming that the body forces are zero, and homogeneous initial conditions are applied, we obtain the boundary integral equation using the Betty's theorem and the full-space fundamental solutions for the displacement and traction components.

In order to consider the material damping of the ballast and the subsoil a complex Young's modulus $\tilde{E} = E(1 + i\omega\beta)$ is applied using the correspondence principle. With the constant coefficient β hysteretic damping is considered in the material.

A numerical discretization of the boundaries leads to a number of algebraic equations

$$\tilde{\mathbf{U}} \tilde{\mathbf{t}} = \tilde{\mathbf{T}} \tilde{\mathbf{u}}, \quad (2)$$

where $\tilde{\mathbf{u}}$ and $\tilde{\mathbf{t}}$ are the complex frequency dependent displacements and tractions at all nodal locations, and $\tilde{\mathbf{U}}$ and $\tilde{\mathbf{T}}$ are the influence matrices. For given tractions the corresponding displacements can be determined. With the inverse transformation the time history of the displacements is defined.

The dynamic behaviour of the rails, the sleepers, the elastic pads, as well as the dynamic property of the neighbouring frame structure can be defined by the equation of motion

$$\mathbf{M}\ddot{\mathbf{u}} + \mathbf{C}\dot{\mathbf{u}} + \mathbf{K}\mathbf{u} = \mathbf{P}, \quad (3)$$

where \mathbf{M} , \mathbf{C} , \mathbf{K} and \mathbf{P} are respectively the mass, damping, stiffness, and nodal force matrix.

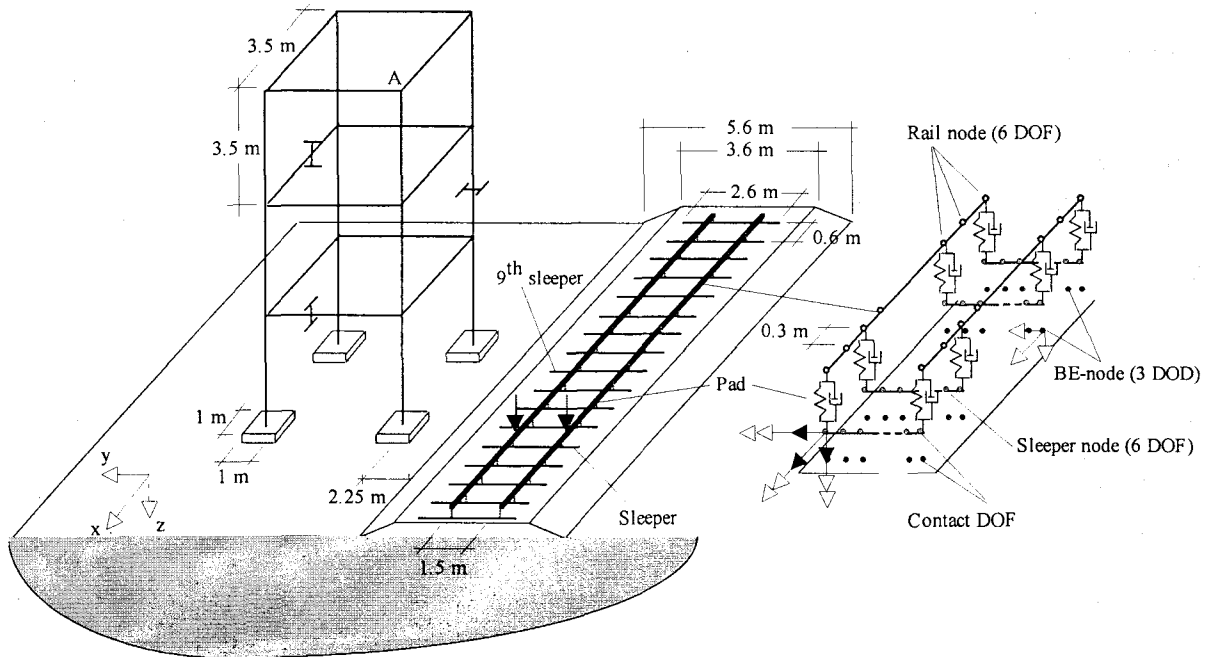


Fig. 1. The considered railway track, subsoil and neighbouring structure system

The equation of motion in the frequency domain is

$$\tilde{\mathbf{K}} \tilde{\mathbf{u}} = \tilde{\mathbf{P}} \quad (4)$$

where the dynamic stiffness of the finite element domain is $\tilde{\mathbf{K}} = \mathbf{K}^R + i \mathbf{K}^i$, and the real and imaginary part of the stiffness are $\mathbf{K}^R = \mathbf{K} - \omega^2 \mathbf{M}$ and $\mathbf{K}^i = \omega \mathbf{C}$, respectively.

In order to couple the FE-domain and the BE-domain, we have to determine the dynamic stiffness of the BE-domain by introducing the matrix \mathbf{A} which includes the area of the boundary elements. The relationship between the nodal forces $\tilde{\mathbf{P}}$ and the displacement $\tilde{\mathbf{u}}$ of the BE-domain at the contact area between the FE-domain and the BE-domain is then obtained by

$$\tilde{\mathbf{K}}^{\text{BEM}} \tilde{\mathbf{u}} = \tilde{\mathbf{P}} \quad (5)$$

with $\tilde{\mathbf{P}} = \tilde{\mathbf{A}} \tilde{\mathbf{t}}$.

The rails and sleepers are discretized with Timoshenko beam elements with shear deformation. The elastic pad comprises an elastic spring and a viscous damper, as indicated in Fig. 1. Each node of the finite elements has six degree-of-freedom (DOFs), three translation DOFs and three rotation DOFs, while each node of the boundary elements has only three translation DOFs. In order to incorporate the dynamic stiffness of the BE-region into the stiffness of the whole system, the rank of the boundary element matrix at the interface nodes has to be expanded to the DOFs of the finite element matrix by inserting zeros at the corresponding rotation DOFs.

The governing equation of the whole system is then

$$\begin{bmatrix} \tilde{\mathbf{K}}_{\text{FF}}^{\text{FEM}} & \tilde{\mathbf{K}}_{\text{FC}}^{\text{FEM}} & 0 \\ \tilde{\mathbf{K}}_{\text{CF}}^{\text{FEM}} & \tilde{\mathbf{K}}_{\text{CC}}^{\text{FEM}} + \tilde{\mathbf{K}}_{\text{CC}}^{\text{BEM}} & \tilde{\mathbf{K}}_{\text{CB}}^{\text{BEM}} \\ 0 & \tilde{\mathbf{K}}_{\text{BC}}^{\text{BEM}} & \tilde{\mathbf{K}}_{\text{BB}}^{\text{BEM}} \end{bmatrix} \begin{bmatrix} \tilde{\mathbf{u}}_{\text{F}} \\ \tilde{\mathbf{u}}_{\text{C}} \\ \tilde{\mathbf{u}}_{\text{B}} \end{bmatrix} = \begin{bmatrix} \tilde{\mathbf{P}}_{\text{F}} \\ \tilde{\mathbf{P}}_{\text{C}} \\ \tilde{\mathbf{P}}_{\text{B}} \end{bmatrix} \quad (6)$$

where the subscript F and B are the finite element and the boundary element area, respectively, and the subscript C indicates the contact DOF (see Fig. 1). Details about the derivation of the numerical procedure are given by Friedrich^{18, 19}.

The moving loads act on the rails as indicated in Fig. 2. Between two sleepers two elements are used for each rail. The time that the loads need to pass the distance d of 0.3 m from one node to the other is determined by the speed v of the moving load.

$$dt = \frac{d}{v} \quad (7)$$

The influence of the moving load on the responses at a certain location k is achieved by superposing the responses due to each loading at the nodes i along the rails

$$u^k(n \, dt) = \sum_{i=1}^n u^i((n-1+1) \, dt) \quad (8)$$

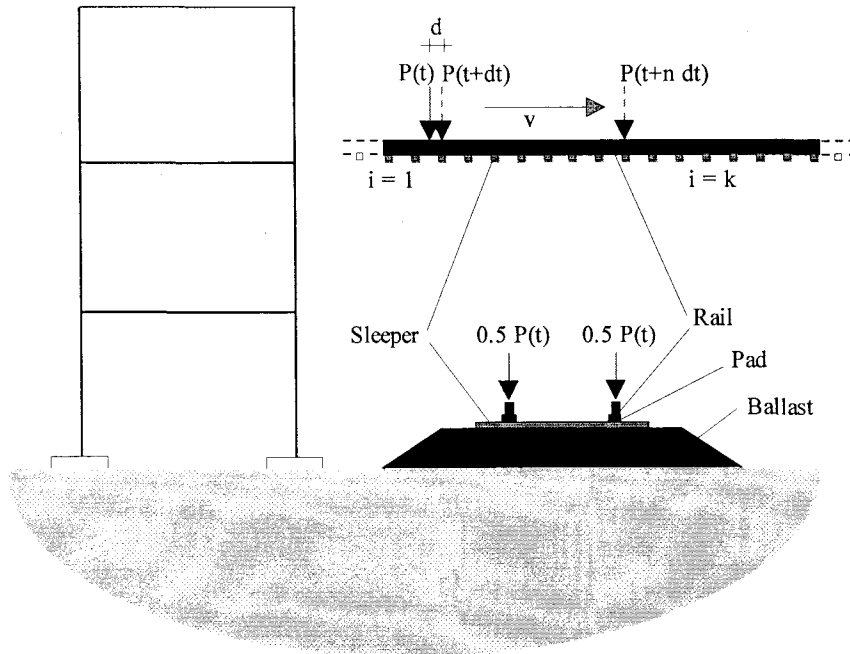


Fig. 2. Moving load on a railway track

3. Numerical results

3.1 Comparative analyses

In order to verify the numerical approach we compare the results with those of other researchers. In the first comparative analyses the steady-state responses of the ground surface due to the vibrations of an embedded foundation are considered. The second case is the vibration of the soil surface induced by a moving point load.

Fig. 3(a) shows the considered system. A rigid foundation is embedded in a half space with the shear wave velocity of 250 m/s, the density of 2000 kg/m³, and the Poisson's ratio of 0.4. It is assumed that the soil has no material damping. The foundation is subjected by a vertical harmonic unit load with the frequency ω . With the amplitude of the steady-state vertical response

$$|U_z| = \sqrt{(U_z^{\text{Real}})^2 + (U_z^{\text{Imaginary}})^2}, \quad (9)$$

the static stiffness K^{static} of the foundation and the load amplitude $P(\omega)$ we can define the dimensionless response amplitude

$$\bar{U}_z = |U_z| \frac{K^{\text{static}}}{P(\omega)} \quad (10)$$

Fig. 3(b) displays the response amplitude as a function of the dimensionless excitation frequency a_0 , which is defined as $\omega b/c_s$, b is the half width of the foundation. The symbol \bullet indicates the result obtained using the current numerical approach, and the symbol \times shows the result by Wolf²⁰ using the scaled boundary finite-element method. The results show that both responses correspond well even though they are obtained by using different methods.

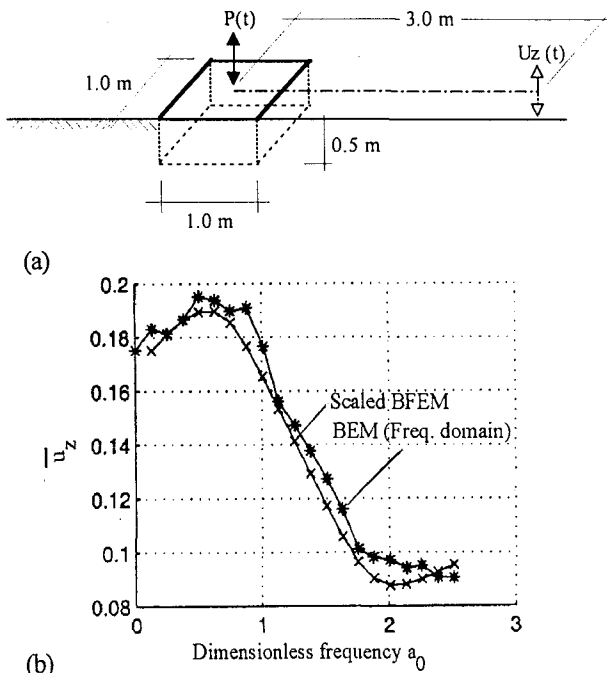


Fig. 3(a) and (b). Vertical ground vibrations due to a vibrating embedded foundation. (a) System and (b) comparative results

Fig. 4(a) shows the surface of a half space with a point load with the amplitude of 1 N moving along a line with the velocity of 180 m/s. The soil has the shear wave velocity of 300 m/s, the density of 2000 kg/m³, and the Poisson's ratio of 0.45. It is also assumed that the soil has no material damping.

Fig 4(b) shows a comparison of the vertical displacement U_z obtained from the presented approach in the frequency domain, with the result of the calculation with a boundary element method¹⁶ direct in the time domain, and the analytical result by Barber²¹. The considered location is 5 m away from the load path. The results of the boundary element calculation in the time and frequency domain correspond very well. While both numerical results begin with a zero value, at time of 0 s the analytical result has a non-zero value. This value is caused by the assumption made in the analytical calculation that the point load starts from infinite distance. In contrast, at the beginning of the boundary element calculations the load is applied suddenly before it moves on the ground surface. This sudden application of the load causes an upward movement at the early phase of the ground displacement time history.

Investigation of the effect of a moving load on railway track on vibrations in a structure in the neighbourhood is not known. A comparison with the results obtained by other researchers is therefore not possible at this moment.

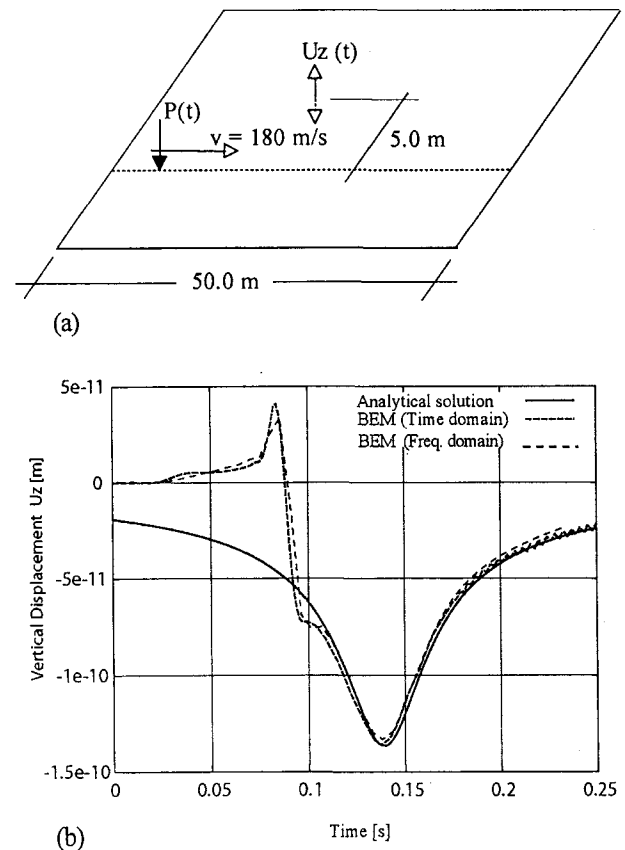


Fig. 4(a) and (b). Vertical ground vibrations due to a moving point load. (a) Considered half space, and (b) comparative results

3.2 Moving load on a half space

In order to investigate the effect of a moving load on the development of ground vibrations with increasing distance a half-space is considered as subsoil. The shear and compressive wave velocity are respectively 120 m/s and 240 m/s, and the density is 2000 kg/m³. It is assumed that the soil has no material damping. Since most traffic loads have a wide range of dominant frequencies above 20 Hz the moving load with a half-sine time history is considered (Fig. 5(a)). The duration of 0.025 s is chosen, so that the wanted frequency content is obtained. The dominant frequencies can be clearly seen in the corresponding response spectrum in Fig. 5(b). The spatial distribution of the load along the load path and the magnitude of the load are modified in such a way that all boundary elements along the load path should experience the same load P_i of 1 MN with the same frequency content as shown in Fig. 5(b). In order to have this load condition, the load distribution has to be longer with increasing load speed. Consequently, the magnitude P_i of the load decreases with the load speed, as indicated in Table 1. The relation between the length l_i of the load distribution and the magnitude P_i of the load is defined through

$$P_i = \frac{P_t \pi}{2 l_i} \quad (11)$$

Table 1. Load distribution alteration with load speed

Load speed [km/h]	Distribution length l_i [m]	P_i [MN/m]
200	1.388	1.1310
300	2.083	0.7540
400	2.778	0.5655
500	3.472	0.4524

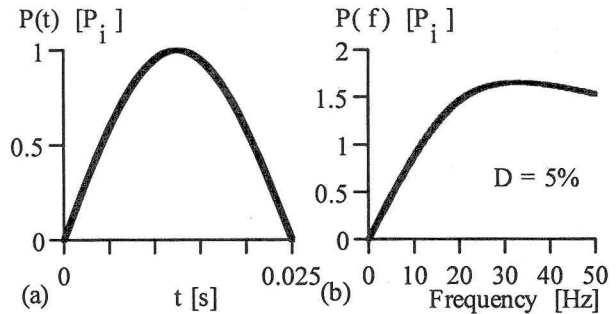


Fig. 5(a) and (b). Moving load on ground surface

Fig. 6 shows the development of the peak ground acceleration PGA along a line perpendicular to the load path with a distance of 18 m from the load entrance boundary.

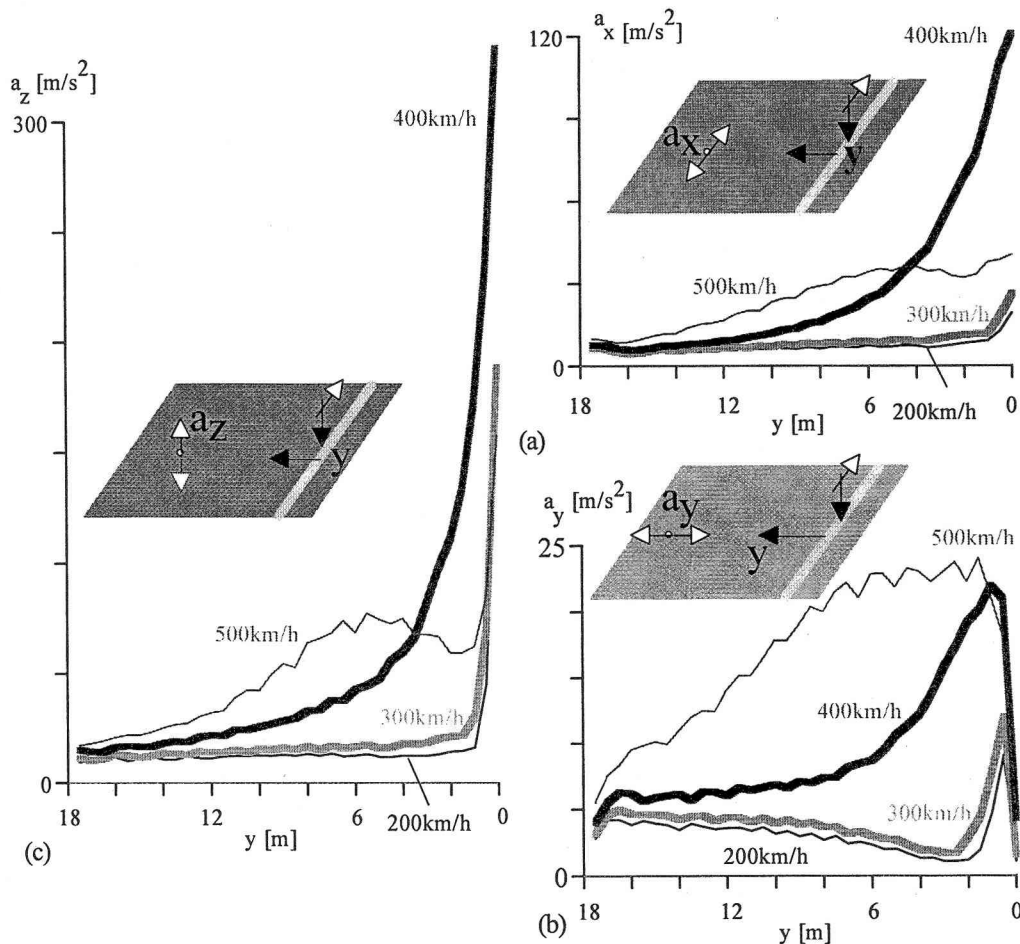


Fig.6(a)–(c). Effect of the speed of the moving load on the peak ground acceleration PGA in the (a) vertical direction, (b) in the direction parallel and (c) perpendicular to the load path

The PGA in the x-direction decreases with an increasing distance from the load path (Fig. 6(a)). At the load path it increases with the load speed, and has the largest value when the load speed is close to the Rayleigh wave speed in the soil. In the considered case this speed has the value of 402 km/h. When the load speed exceeds the wave speed the PGA decreases again.

The PGA in the y-direction first increases, and then becomes smaller with an increasing distance from the load path (Fig. 6(b)). At the load path it should have a zero value due to the symmetrical wave propagation. The existing calculated values at the load path are caused by the considered unsymmetrical region. When the load speed exceeds the Rayleigh wave speed the PGA becomes the largest compared to the PGA due to other considered load speeds, and the decrease with the distance from the load path also occurs slower.

In the vertical direction the PGA at the load path changes drastically with the load speed (Fig. 6(c)). In the vicinity of the load path the development is similar to the PGA in the direction parallel to the load path. For the response of a structure to the ground motions the PGA is not the only important factor. The frequency content of the ground excitation is also essential (Chouw and Pflanz¹).

3.3 Moving load on a railway track

In order to investigate the influence of a load moving along a railway track on the development of ground vibrations at the track itself and the surrounding area the system in Fig. 1 is considered. The length of the modeled rails and sleepers is 9.6 m and 2.6 m, respectively. The rail distance is 1.5 m. The width and height of the sleepers are 0.26 m and 0.2 m, respectively.

The sleeper has a mass of 290 kg, a Poisson's ratio of 0.16, and a Young's modulus of $3.0 \cdot 10^6 \text{ N/m}^2$. The moment of inertia of the cross-section area and the Young's modulus of the rail are $3.055 \cdot 10^{-5} \text{ m}^4$ and $2.1 \cdot 10^{11} \text{ N/m}^2$, respectively. The cross-section and the Poisson's ratio of the rail are $7.686 \cdot 10^{-3} \text{ m}^2$ and 0.3, respectively. The rail pad has the stiffness and the damping constant of $6 \cdot 10^8 \text{ N/m}$ and $2 \cdot 10^4 \text{ Ns/m}$, respectively. The shear wave velocity of the subsoil and the ballast is 200 m/s and 300 m/s, respectively. They have the same density of 1700 kg/m^3 and the same Poisson's ratio of 0.25. The material damping of the ballast is 3%. It is assumed that the subsoil has no material damping. The ballast has the upper and bottom width of 3.6 m and 5.6 m, respectively.

The characteristic of the load is given in Fig. 7 as a function of the ratio of the impulse duration td . Fig. 7(b) shows the corresponding response spectrum with no damping. T_n is the considered period of the single-degree-of-freedom (SDOF) system. The excitation is considered as loads at the rail nodes. With increasing speed the time dt that the loads need to pass the distance between two rail nodes becomes shorter. For the considered load speeds v of 108 km/h, 180 km/h, and 288 km/h the time dt becomes 0.01 s, 0.006 s and 0.0038 s, respectively.

dt is also equal the impulse duration td that the loads will act on the rails.

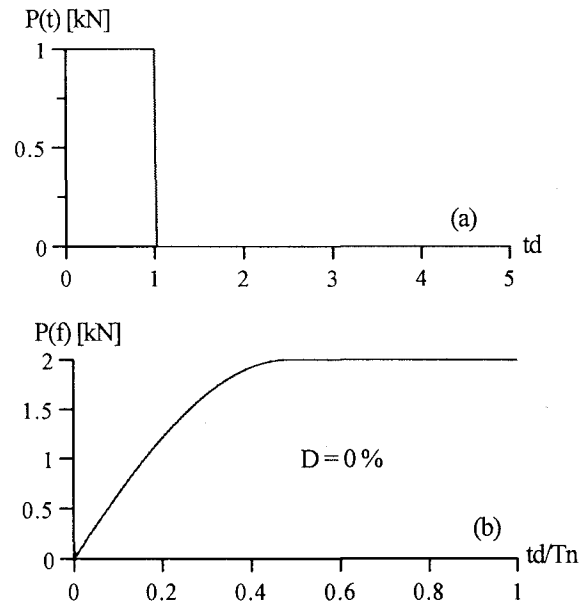


Fig. 7(a) and (b). Moving load.
(a) Time history, and (b) response spectrum

Fig. 8 shows the development of the amplitude of the vertical steady-state displacement of the rail and the ballast due to a unit harmonic load at the middle sleeper (the 9th sleeper). Due to the considered soft rail pad the rails experience a larger displacement than the ballast.

In Fig. 9 the influence of the load speed on the vertical displacement of the rails and the ballast beneath the 9th sleeper is displayed. Corresponding to the speed the response occurs earlier with a higher load speed. The time 0 s is the time when the load acts on the first rail node. However, since the load speed is much slower than the wave speed of about 2950 m/s or 10620 km/h in the rails and also lower than the wave velocity in the ballast and the subsoil, no strong amplification is expected as in the previous considered case of the ground vibrations when the moving load acts directly on the soil surface (see Fig. 6). Corresponding to the frequency response in Fig. 8 the rails experience a larger displacement than the ballast. Because of the shorter contact between the loads and the rails (Eq. 7) the rails as well as the ballast have shorter duration in their response with increasing load speed.

Fig. 10(a) and (b) show the response spectrum of the vertical induced acceleration at the ballast beneath the 9th sleeper and at the surrounding ground surface, 3.75 m away from the left end of the 9th sleeper (see Fig. 1). The considered damping ratio is 5%. As we can see from Fig. 7(b) the loads have a constant response spectrum value at the boundary frequency 40 Hz, 66.6 Hz, and 105.3 Hz, when the load speed is 108 km/h, 180 km/h, and 288 km/h, respectively. The response spectra in Fig. 10(a) represent the effect of the ground motions at the

ballast. The responses show that after a certain frequency the response spectrum values oscillate around a certain constant value. The amplitude of the response spectrum oscillation increases with the load speed. The frequency, when the response spectrum value starts to oscillate, has also higher value with an increasing load speed. However, these frequencies are much

lower than the corresponding boundary frequencies of the loads. While the loads have the same maximum response spectrum value, the maximum response spectrum values of the ballast vibrations decrease with a lower load speed. At the ground in the vicinity of the railway track the induced ground accelerations have similar frequency content, however, the magnitude is much smaller (Fig. 10(b)).

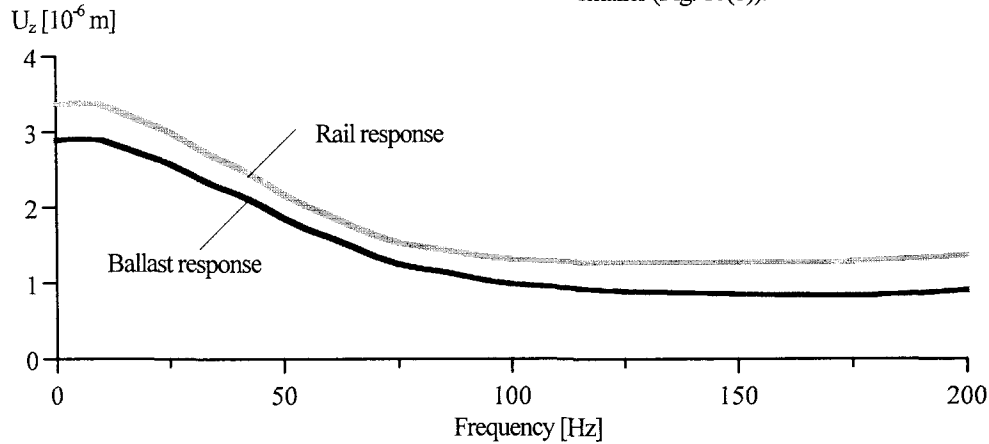


Fig. 8. Amplitude development of the steady-state vertical displacement at the middle sleeper with load frequency

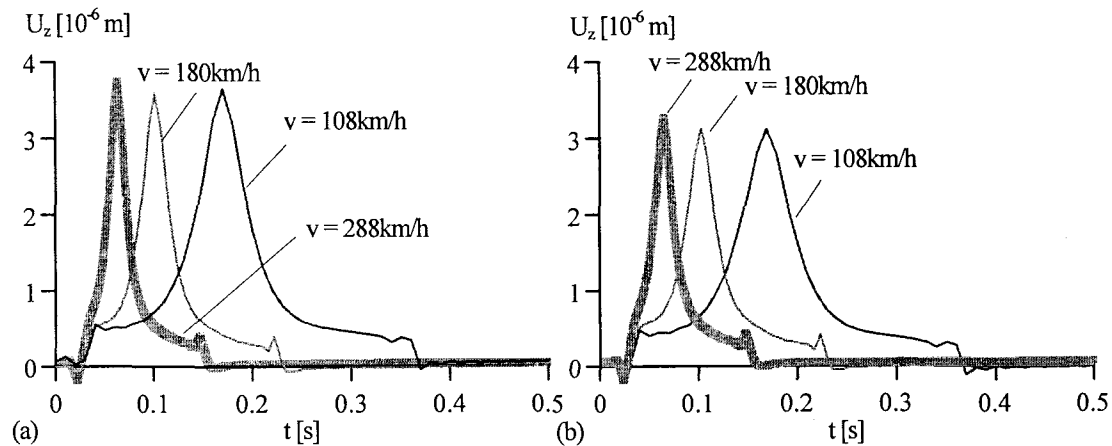


Figure 9(a) and (b). Influence of the load speed on the vertical displacement of (a) the rail and (b) the ballast at the middle sleeper

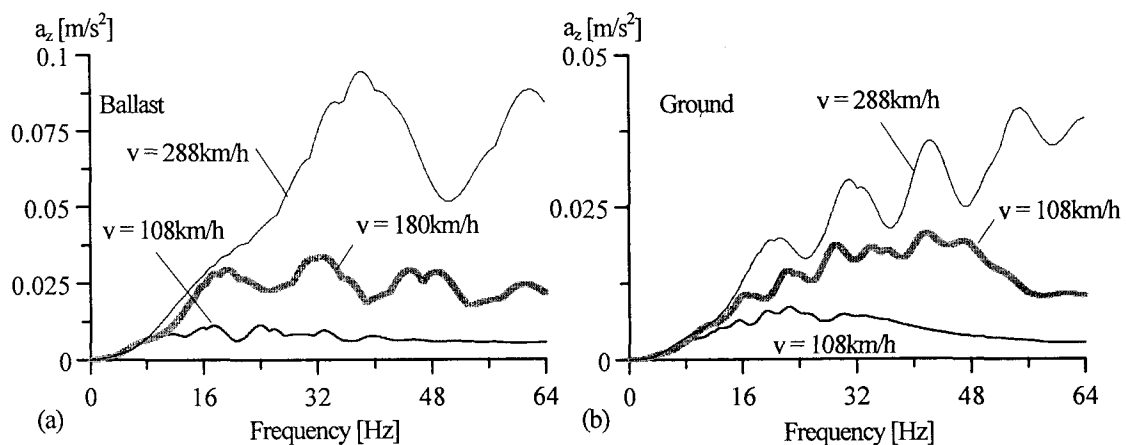


Figure 10(a) and (b). Influence of the load speed on the induced ballast and surrounding ground vibrations

3.4 Structural vibrations in the neighbourhood

In order to investigate the influence of the moving load on structures in the surrounding of the railway track a three-dimensional steel frame structure is considered.

Each member of the frame structure has a length of 3.5 m, and a mass per unit length is 74.4 kg/m. The flexural stiffness EI_y is 4921.214 kNm², and EI_z is 34438.95 kNm². The torsional constant I_p is $7.4 \cdot 10^{-7}$ m⁴. EA is 1991619 kN. The orientation of the double T-profile of the steel structural members is shown in Fig. 1. The local y- and z-axis is the axis perpendicular and parallel to the flange, respectively. Each node of the structural member has 6 DOFs. The surface foundations have a dimension of 1 m x 1 m x 0.4 m (see Fig. 1). It is assumed that the foundations are rigid and consist of reinforced concrete. The material damping of the structural members is described by a complex modulus of elasticity, which is governed by the Kelvin parameters E_1 and E_n (Hashimoto and Chou²²). The advantage of this damping model is that the structure has almost frequency independent material damping. For the chosen value $E_1 = 0.1$ and $E_n = 10^{28}$ the equivalent damping ratio is about 1.4%.

The fundamental frequency of the natural structural vibration in the direction parallel and perpendicular to the railway track is 3.29 Hz and 6.26 Hz, respectively. The chosen

orientation of the double T-steel-profile results in a higher fundamental frequency of the structural vibration in the direction perpendicular to the railway track. Fig. 11 shows the influence of the load speed and the direction of the considered ground motions on the response spectrum values of the induced accelerations at the top corner A of the structure (see Fig. 1). The considered damping ratio is 5 %. The results in Fig. 11(a) are caused by a simultaneous ground motions. The induced structural vibrations increase with the increasing load speed.

In earthquake engineering it is common to consider the horizontal ground motions in the design of the structure. The reason is that the horizontal earthquake ground motions have generally low dominant frequencies, and the structural fundamental frequency normally belongs to the global vibration of the structure in the horizontal direction.

In the earthquake design in general the vertical ground motions may be neglected. In contrast, in the case of man-made ground vibrations it is commonly believed that the vertical ground motions are the most significant loads for the structural design. In order to investigate the influence of the excitation direction the response of the structure to each component of the ground excitation is considered.

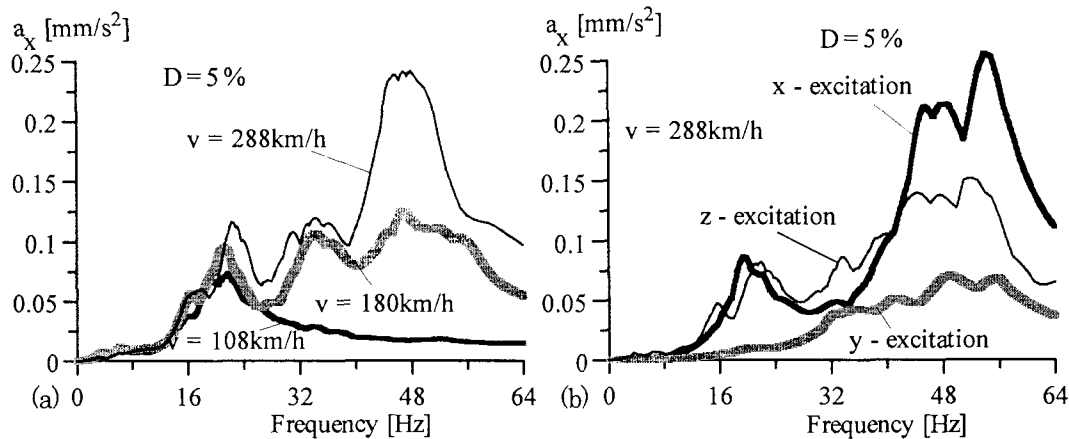


Fig. 11(a) and (b). Influence of the load speed and the direction of the ground excitation on the induced accelerations in the x direction at the location A

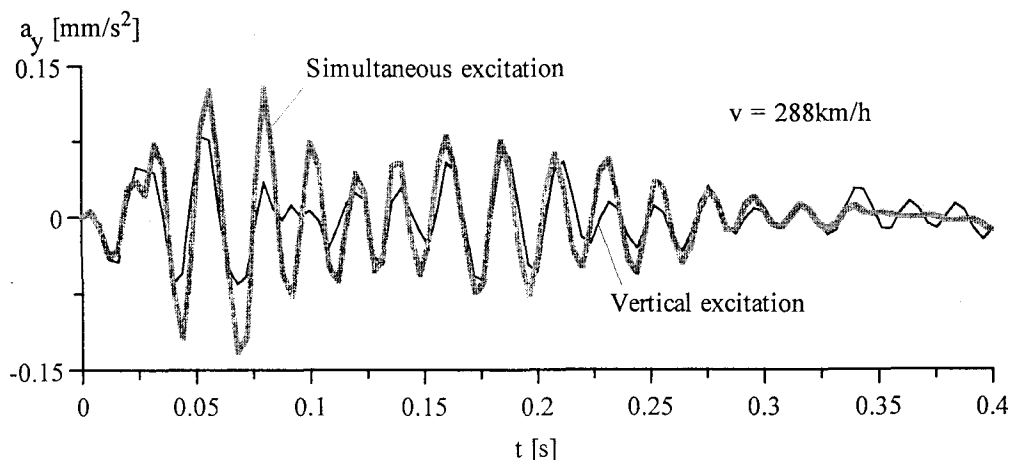


Fig. 12. Influence of a simultaneous excitation on the induced accelerations in the y direction at the location A

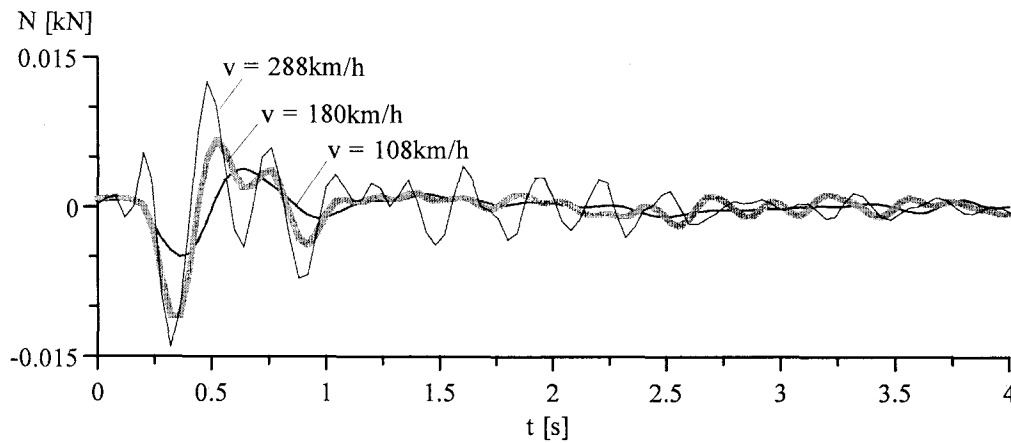


Fig. 13. Effect of the load speed on the axial forces N in the upper column below A

Fig. 11(b) shows that as expected the response in the x-direction is strongly determined by the ground motions in the x-direction, and the y-component has much smaller influence. The vertical ground motion has slightly larger influence in a limited frequency range. In most of the considered frequency range the influence of the vertical ground motion is smaller than the x-component excitation.

Fig. 12 shows the effect of a simultaneous ground motion on the induced accelerations in the y-direction at the location A of the structure. A comparison with the response due to the vertical ground motions clearly shows that a consideration of the vertical ground vibrations alone can underestimate the activated induced vibrations in the structure. Consequently, the excitation of secondary structures, which are attached to the structural members of the main structure, can be underestimated as well.

Fig. 13 shows that corresponding to the vertical surrounding ground vibrations the activated axial forces increase with increasing load speed. The axial forces, tensile and compressive forces, in the columns occur in the case of horizontal ground excitations mainly due to the excited fundamental modes in the horizontal direction. In the case of vertical ground excitation they occur due to a direct excitation of all columns. Because of the participating railway track in the wave propagation effect, the speed of the moving loads cannot be compared with the speed of the Rayleigh waves in the ground as in the purely half-space case. It is still not clear how the rails, elastic pads, the sleepers and the ballast affect the wave propagation into the surrounding ground. In order to clarify this effect further investigations are necessary.

4. Conclusions

In this work a numerical approach for a simulation of the vibrations of a railway track, the wave propagation into the surrounding of the track and neighbouring structures is introduced. In the simulation the track, the neighbouring structure and its foundations are described by a finite element method, and the soil that links the track with the adjacent structure

is described by a boundary element method. The calculation is performed in the frequency domain. The time histories of the structural response are obtained with the help of the Fourier transformation.

The simulation procedure can be used for predicting the occurring ground and structural vibrations due to a passing train in the neighbourhood. It is significant for the preparation of a planned construction and also for the prediction of the durability of the railway tracks.

The investigation of the considered cases reveals that the nature of the ground excitation is ignored if only the vertical component of the ground motions is considered. Since a structure always experiences vertical as well as horizontal ground motions simultaneously, the structural response to the ground motions induced by the loads on the railway track depends not only on the characteristic of the vertical but also on the horizontal ground motions. In order to obtain a more realistic result it is necessary to consider the simultaneous ground excitation.

Acknowledgments

The authors greatly appreciate the valuable comments by the reviewers that significantly improved the clarity of the article.

References

- 1) Chouw, N., Pflanz, G. Reduction of structural vibrations due to moving load. *Proceedings of the 2nd int. workshop WAVE2000*, Bochum, Germany. pp. 251-268. Rotterdam: Balkema, 2000.
- 2) Chouw, N., Schmid, G. (Eds.) *International workshop WAVE2002 wave propagation, moving load and vibration reduction*, ISBN 9058095592, Swets & Zeitlinger B.V., Lisse, 271 pp., 2003.
- 3) Krylov, V. V., Vibration impact of high-speed trains. Effect of track dynamics. *J. Acoust. Soc. Am.* Vol. 100(5), pp. 3121-3133, 1996.
- 4) Pan, G., Atluri, S. N., Dynamic response of finite

- sized elastic runways subjected to moving loads: A coupled BEM/FEM approach. *J. Numer. Meth. Eng.*, Vol. 38, pp. 3143-3166, 1995.
- 5) Petyt, M., Jones, C., Modeling of ground-borne vibration from railways, *Proc. of EURODYN*, Vol. 1, pp. 79-87, 1999.
 - 6) Lefeuvre-Mesgouez, G., *Propagation d'ondes dans un massif soumis à des charges se déplaçant à vitesse constante*. Dissertation, Ecole Centrale de Nantes, 1999.
 - 7) Hirschauer, R., *Kopplung von Finiten Elementen mit Rand-Elementen zur Berechnung der dynamischen Baugrund-Bauwerk-Interaktion*. Dissertation, T. U. Berlin, 2001.
 - 8) Waas, G., *Linear two-dimensional analysis of soil dynamics problems in semi infinite layered media*. Dissertation, U. C. Berkeley, 1968.
 - 9) Kausel, E., Thin-layer method: formulation in the time domain. *J. Numerical Eng. Mechanics*, Vol. 37, pp. 927-941, 1994.
 - 10) Mohammadi, M., Karabalis, D., Dynamic 3-D soil-railway track interaction by BEM-FEM. *Earthquake Engineering and Structural Dynamics*, Vol. 24, pp. 1177-1193, 1995.
 - 11) Zhu, X. Q., Law, S. S., Precise time-step integration for the dynamic response of a continuous beam under moving loads. *J. of Sound and Vibration*, Vol. 240(5), pp. 962-970, 2001.
 - 12) Savin, E., Dynamic amplification factor and response spectrum for the evaluation of vibrations of beams under successive moving loads. *J. Sound and Vibration*, Vol. 248(2), pp. 267-288, 2001.
 - 13) Chen, Y. H., Huang, Y. H., Shih, C. T., Response of an infinite Timoshenko beam on a viscoelastic foundation to a harmonic moving load. *J. Sound and Vibration*, Vol. 241(5), pp. 809-824, 2001.
 - 14) De Barros, F. C. P., Luco, J. E., Response of a layered viscoelastic half-space to a moving point load. *Wave Motion*, Vol. 19, pp. 189-210, 1994.
 - 15) Yang, Y.-B., Hung, H.-H., A 2.5D finite/infinite element approach for modelling visco-elastic bodies subjected to moving loads, *J. Numer. Method Eng.*, Vol. 51, pp. 1317-1336, 2001.
 - 16) Pflanz, G. Numerische Untersuchung der elastischen Wellenausbreitung infolge bewegter Lasten mittels der Randelementmethode im Zeitbereich. *VDI Fortschritt-Berichte Reihe 18*, Nr. 265, VDI Verlag, Düsseldorf, 2001.
 - 17) Pflanz, G., Hashimoto, K., Chouw, N. Reduction of structural vibrations induced by a moving load. *Journal of Applied Mechanics*, Vol. 5, pp. 555-563, 2002.
 - 18) Friedrich, K. *Einfluß der Bauwerk-Baugrund-Wechselwirkung auf das dynamische Verhalten des Eisenbahnoberbaus*, Ruhr University Bochum, Ph.D. Thesis, 2003.
 - 19) Friedrich, K., Schmid, G. Dynamic behaviour of railway track systems analyzed in frequency domain, *Lecture Notes in Applied Mechanics*, Vol. 6, pp. 377-394, Springer Verlag, 2003.
 - 20) Wolf, J. P. Far-field displacements of 3-D soil in scaled boundary finite-element method, *Proceedings of the 2nd int. workshop WAVE2000*, Bochum, Germany. pp. 421-430. Rotterdam: Balkema, 2000.
 - 21) Barber, J. R. Surface displacements due to a steadily moving point force. *Journal of Applied Mechanics*, Vol. 63, pp. 245-251, 1996.
 - 22) Hashimoto, K., Chouw, N. Investigation of the effect of Kobe earthquake on a three-dimensional soil-structure system. *Journal of Earthquake Engineering*, Vol. 27, pp 1-8, 2003.

(Received: April 16, 2004)